Heliyon 10 (2024) e23661

Contents lists available at ScienceDirect

Heliyon

journal homepage: www.cell.com/heliyon

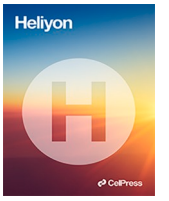

Comprehensive analysis of the role of cuproptosis-related genes in the prognosis and immune infiltration of adrenocortical Carcinoma

Zhiyuan You [a,*], Jiqing He [b], Zhongming Gao [c]

[a] School of Clinical Medicine, Hangzhou Normal University, Hangzhou, 310005, China
[b] Department of Obstetrics, The Affiliated Hospital of Hangzhou Normal University, Hangzhou, 310005, China
[c] Department of Neurology, The Affiliated Hospital of Hangzhou Normal University, Hangzhou, 310005, China

ARTICLE INFO

Keywords:
Cuproptosis
Adrenocortical carcinoma
Cancer therapy
Immune checkpoint inhibitor
Immune infiltration
Cancer prognosis

ABSTRACT

Background: Cuproptosis is a recently discovered form of nonapoptotic programmed cell death. However, no research on cuproptosis in the context of adrenocortical carcinoma has been conducted, and the prognostic value of assessing cuproptosis remains unclear.
Methods: In this study, we established comprehensive models to assess gene expression changes, mutation status, and prognosis prediction and developed a prognostic nomogram for cuproptosis-related genes. Using data from The Cancer Genome Atlas (TCGA), Gene Expression Omnibus (GEO), and Genotype-Tissue Expression (GTEx) databases, an analysis of 11 cuproptosis-related genes was performed. Additionally, a risk scoring method and nomogram were used to assess the relationships among cuproptosis-associated genes, transcript expression, clinical characteristics, and prognosis. The connections among tumors, immune checkpoints, and immune infiltration were also analyzed.
Results: The patterns observed in patients with adrenocortical carcinoma who were assessed using cuproptosis-associated risk scores provide useful information for understanding gene mutations, clinical outcomes, immune cell infiltration, and immune checkpoint analysis results. *FDX1*, *LIPT1*, *MTF1*, *COX11*, *CYP2D6*, *DLAT*, *ATP7B*and *CDKN2A* were differentially expressed in patients with adrenocortical carcinoma and normal controls. In addition, higher risk scores were significantly associated with poor overall survival and progression-free interval. The nomogram model subsequently developed to facilitate the clinical application of the analysis showed good predictive and calibration capabilities. GSE10927 and GSE33371 were used for independent cohort validation. Moreover, *CDKN2A*, *FDX1*, and other cuproptosis-related genes were significantly associated with immune infiltration and checkpoints.
Conclusion: We confirmed that our model had excellent predictive ability in patients with adrenocortical carcinoma. Therefore, an in-depth evaluation of patients using cuproptosis-related risk scores is clinically essential and can assist in therapy in the future.

* Corresponding author.
E-mail address: 2019211301074@stu.hznu.edu.cn (Z. You).

https://doi.org/10.1016/j.heliyon.2023.e23661
Received 4 April 2023; Received in revised form 23 November 2023; Accepted 9 December 2023
Available online 14 December 2023
2405-8440/© 2023 The Authors. Published by Elsevier Ltd. This is an open access article under the CC BY-NC-ND license (http://creativecommons.org/licenses/by-nc-nd/4.0/).

1. Introduction

Adrenocortical carcinoma (ACC) is a rare and exceedingly aggressive malignancy. Its annual incidence ranges from 0.7 to 2.0 cases per million population [1]. The pathogenesis of ACC remains unclear. Studies have shown that insulin-like growth factor 2 (IGF2) overexpression and abnormal activation of β-catenin are significantly correlated with the clinical progression of ACC [2,3]. Recent genome-wide studies on ACC have contributed to the understanding of the disease, but diagnosing ACC remains a challenge [4]. A study by Cheng et al. [4] showed that patients with ACC are often diagnosed at an advanced stage when treatment options are limited. According to a substantial number of epidemiological studies, 50 % of deaths from ACC occur within 2 years after the appearance of symptoms, and the 5-year survival rate is less than 35 % [4–7]. Therefore, due to the high morbidity and mortality of ACC, there is a pressing need to develop an efficient prognostic model that can provide a more in-depth understanding of ACC.

Copper is an essential trace element for humans. In the human body, copper has vital physiological features that affect the absorption and utilization of iron and the synthesis of hemoglobin and pigments. It participates in various biochemical reactions and plays an essential role in the body's redox compartment, endocrine function, metabolism, and neurotransmitter formation [8]. Copper levels are drastically altered in the tissues and blood of most persons with cancer compared to healthy people [9–13]. It is apparent that copper disorders cause toxicity to cells and that intracellular copper levels may have a critical impact on cancer development [12]. Similarly, in a previous study, we found that cancer cell treatment with copper ion complexes via the activation of mitogen-activated protein kinase pathway-induced cellular oxidative stress eventually led to cell death [14]. All these findings show the overall effect of copper ions.

Studies have identified different types of cell death, such as necroptosis, ferroptosis, and pyroptosis, which are considered necrotic programmed cell death [15,16]. However, a recent study revealed another previously undiscovered mechanism for regulating cell death [17]. Tsvetkov et al. [18] observed that highly aerobic cells are nearly 1000-fold more sensitive to copper ionophores than cells undergoing glycolysis. Copper does not directly affect the mitochondrial electron transport chain but inhibits the tricarboxylic acid (TCA) cycle in the mitochondria [18]. On the basis of this theory, Tsvetkov et al. [18] found that when copper ions accumulate excessively in cells dependent on mitochondrial respiration, they can bind directly to the recombinant dihydrolipoyl transacetylase (DLAT) of the tricarboxylic acid cycle (TCA), contributing to abnormal denaturation and cell death. This provided a solid foundation for subsequent related studies. Moreover, copper ions can reduce the level of the Fe–S cluster. These mechanisms cause a proteotoxic stress response that ultimately leads to cell death. Therefore, several copper-related anticancer drugs have been applied in clinical treatment, such as copper ionophores (dithiocarbamates and disulfiram) and copper chelators [19,20].

Wang et al. [21], Cai et al. [22], Yuan et al. [23] and Xin et al. [24] comprehensively studied the association that exists between cuproptosis genes such as *FDX1* and renal clear cell carcinoma, which plays a crucial role in tumorigenesis as well as tumor growth and metastasis. Their study demonstrated a significant impact of cuproptosis-related genes (CRGs) on the prognosis of renal clear cell carcinoma, with higher risk scores associated with worse prognosis. CRGs were shown to have a similar role in different subtypes of renal cancer [25–27]. For instance, *FDX1* and other genes are downregulated in advanced cancers and influence disease progression through key molecular functions and pathways. *DLAT* acetylates the k76 site of 6-phosphogluconate dehydrogenase, and *CYP2D6* regulates protein reduction, which in turn regulates intracellular copper levels [28–31]. Different CRGs are significantly associated with disease prognosis and immune cell infiltration. CRGs have also been shown to be valuable in other types of cancer research, such as colorectal, lung, and bladder cancers, which provides a theoretical basis for our study [28–31].

The exact relationship between ACC and cuproptosis must be fully understood, and identifying CRGs will play an essential role in improving the survival of patients with ACC. To investigate the relevant role of cuproptosis in ACC, we identified CRGs and examined their relationships with prognosis. Our study investigated the correlation between CRGs and scientific aspects, focusing on the relationship between two associated genes (*FDX1* and *CDKN2A*) and prognosis. Based on these genes, we constructed a prognostic model for ACC. In addition, extensive variations were found in metabolic pathway analysis, immune infiltration analysis, and so on. Our model is highly practicable to guide the staging and treatment of patients with ACC, demonstrating its clinical value and relevance.

2. Materials and methods

2.1. Data sources

Data were accessed from The Cancer Genome Atlas (TCGA; https://www.cancer.gov/) and the Gene Expression Omnibus (GEO; https://www.ncbi.nlm.nih.gov/geo/) databases. The RNA expression statistics in our study were acquired from the TCGA-ACC database. We also selected two datasets from the GEO cohorts, GSE10927 [32] and GSE33371 [3], for data validation. A total of 79 patients with ACC and 128 normal tissues from the Genotype-Tissue Expression (GTEx) database (https://www.gtex-portal.org/) were included in our study [33]. From the raw data, STAR was used to measure the level of gene expression, which we subsequently transformed into transcripts per million. Clinical data collected from TCGA included survival time, survival status, sex, age of onset, tumor grade, and disease stage. All the data and clinical information in this study were retrieved from public databases. Therefore, ethics committee approval and written informed consent were not necessary.

2.2. Identification of CRGs and mapping the correlation

Our study was based on a series of studies by Tsvetkov et al. [18], Wang et al. [34], and Zhang et al. [35]. Referring to a previous study [34] that included 41 CRGs in a univariate Cox analysis, our study identified cuproptosis-related factors with a significant

association with ACC ($p < 0.1$). Subsequently, we screened for more valuable prognostic factors by least absolute shrinkage and selection operator (LASSO). We compiled and selected some genes closely associated with cuproptosis based on previous literature and the GeneCards database for our analysis. In addition, we acquired mRNA expression statistics from the TCGA database and characterized the correlation within the gene set in ACC. We used the R package "ggplot2" for visualization. Spearman correlation evaluation was performed to describe the relationship among the CRGs. A P value < 0.05 was considered to have relevance, and a P value < 0.01 indicated a significant association. In addition, we selected two of the highest correlated genes for a scatter diagram analysis using the same method described earlier.

2.3. Differential CRG expression analysis and validation

Our study determined the differential gene expression of CRGs between standard samples and tumor tissue samples from patients with ACC. We used the Mann–Whitney *U* test to analyze the samples. The data were considered statistically significant and correlated for $P < 0.05$. To verify that samples derived from different patients with ACC tissues did exhibit these gene expression differences, we selected 130 samples from two sets of ACC data [GSE10927 [32], GSE33371 [3]] on the GEO website. These two datasets were generated using the Affymetrix Human Genome U133 Plus 2.0 Array (GPL570). We selected four genes for differential validation based on their relationship with cuproptosis and their importance. The R package "ggplot2" was used to plot the expressions. After a selective analysis of expression differences, we identified the genes with significant variations among separate samples for further analysis.

2.4. Gene mutation profile map

Gene copy-number alterations (CNAs) are hallmarks in the cancer genome and are significant somatic genomic variants that contribute to tumorigenesis. We used the publicly available website cBioPortal for Cancer Genomics to generate cuproptosis gene mutation profile maps [3]. The cBioPortal for Cancer Genomics is a platform developed by the Memorial Sloan Kettering Cancer Center that combines data mining, integration, and visualization based on the TCGA database. Its software is available from GitHub.

2.5. Gene network and Gene Ontology/Kyoto Encyclopedia genes and genomes enrichment analysis of CRGs

To identify potential interactions of CRGs, the GENEMANIA website was used to generate gene network maps for analysis [36]. For pathway enrichment, we used the R package "clusterProfiler" [37]. The R package "org.Hs.eg.db" was used for ID conversion. We used the Benjamini–Hochberg method to perform multiple corrections on the data. Gene Ontology (GO) and the Kyoto Encyclopedia of Genes and Genomes (KEGG) were used as references for our enrichment analysis [38,39]. Differentially expressed CRGs in the high- and low-risk groups were analyzed.

2.6. Development and validation of the CRG risk score

We reviewed the overall survival (OS) data and data involving the eight CRGs from the univariate Cox analysis model and included the genes with $p < 0.1$ (*FDX1*, *CDKN2A*, *LIPT1*, *CYP2D6*, *DLAT*) in the multivariate analysis. We finally found that differences in *CYP2D6* and *CDKN2A* levels were statistically significant in the multivariate Cox analysis ($p < 0.05$) using the R package "survival". We performed the same univariate and multifactor analyses using the progression-free interval (PFI) data and data involving CRGs, and the results showed that the findings regarding *CDKN2A* and *CYP2D6* were still statistically significant.

Based on the above conclusions, we selected two CRGs, *CDKN2A* and *CYP2D6*, for the construction of the CRG risk score (CRRS) model. We calculated the hazard ratios (HRs) for OS and PFI as follows: CRRS = volume of each cuproptosis-associated mRNA expression × corresponding correlation coefficient. With the R package "survival", we plotted Kaplan–Meier survival curves for the high- and low-risk groups of *CYP2D6* and *CDKN2A*, including OS and PFI data. The R package "survminer" was used for visualization. Receiver operating characteristic (ROC) curves were used to visualize predictive capability; the R package "timeROC" was used for the analysis, and "ggplot2" was used for visualization.

2.7. Construction and validation of the nomogram

Based on the crucial role of *FDX1* and *CDKN2A* in copper metabolism and their strong association with the prognosis of ACC patients, we included CRG expression, pathological stage, and age of onset in the evaluation for possible differences. We then constructed a hybrid nomogram using the R packages "rms" and "rmda" to predict OS. We also used time-dependent ROC curves and data calibration curves to predict the accuracy of the nomogram. The prediction was indicated by the areas under the curve (AUCs) and the fit of the calibration curve. Moreover, we calculated the consistency index (C-index) to determine the validity of the OS calibration curves. The C-index varies from 0.5 to 1.0, and a higher C-index indicates a stronger predictive power of the forecasting model. Additionally, to prevent overfitting our established model, we used data from two datasets, GSE33371 and GSE10927, for external validation.

2.8. Analysis of correlation with immune Infiltration

We used the Tumor Immune Estimation Resource (http://timer.cistrome.org/) system to assess the clinical impact of the different

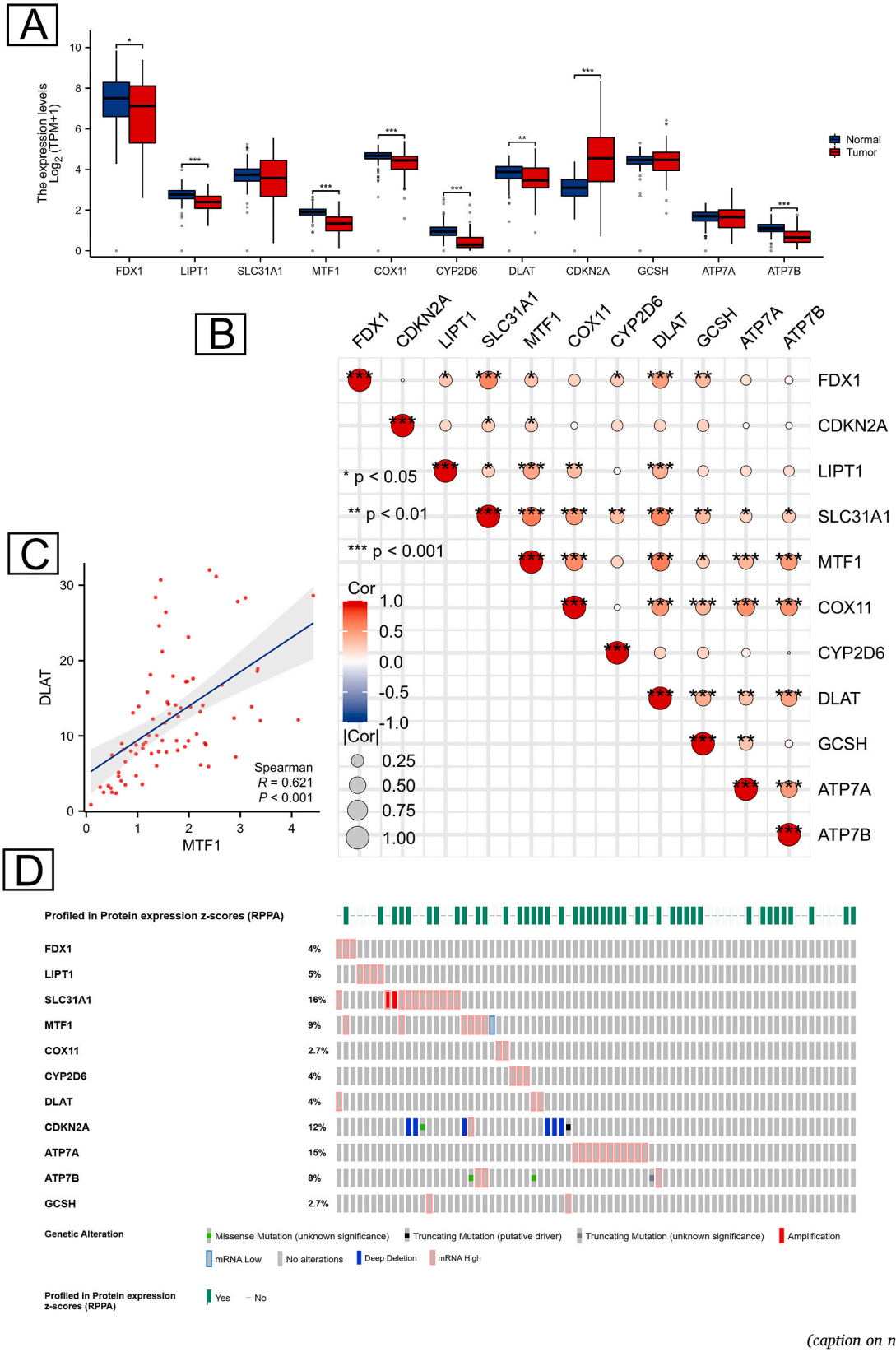

(caption on next page)

Fig. 1. Differential expression and mutations of the CRGs in ACC. (**A**) The different expression levels of the 11 CRGs in ACC and normal tissue samples. The central line represents the median value, and the upper and lower lines represent the quartile values. (**B**, **C**) The correlation between the transcription of the CRGs, with a negative correlation indicated in blue and a positive correlation indicated in red. (**D**) The genetic changes in the 10 CRGs. *P < 0.01, **P < 0.005, ***P < 0.001. CRG: cuproptosis-related gene; ACC: adrenocortical carcinoma, TPM: transcripts per kilobase of exon model per million mapped reads. (For interpretation of the references to color in this figure legend, the reader is referred to the Web version of this article.)

immune cells in patients with ACC [40]. Our study included six types of immune cells (B cells, $CD8^+$ T cells, $CD4^+$ T cells, macrophages, neutrophils, and dendritic cells) [41] and examined four necessary immune checkpoints, including PD-1, PD-L1, TIM-3, and CTLA-4. This investigation was an immune checkpoint inhibitor (ICI) evaluation performed through TISIDB (http://cis.hku.hk/TISIDB/) [42]. According to the results, the expression levels of these genes were associated with the efficacy of immunosuppressive drugs [34,43].

3. The results

3.1. Identification of CRGs

We referred to several past studies and selected a total of 41 genes associated with cuproptosis (Fig. S1 A). We performed univariate and multivariate Cox regression analyses of these 41 genes to identify key genes associated with cuproptosis. Using univariate Cox regression, we identified CRGs that were significantly associated with prognosis ($p < 0.1$) and included them in LASSO analysis. *CDKN2A*, *CYP2D6*, *DLAT* and *SLC31A1* were considered significant features (figure S1 B-C). Subsequently, we used the GeneCards (https://www.genecards.org/) website and Harmonizome website to select 2114 genes associated with ACC. According to the National Center for Biotechnology Information website (https://www.ncbi.nlm.nih.gov/), we also found that *LIPT1* is strongly correlated with lipoic acid transport, *MTF1* is a metal transcription regulator, and *COX11* has a molecular chaperone role for cytochrome C, all of which are closely associated with copper metabolism, so we considered them in the model. The remaining cuproptosis-related genes are also of great importance and have been reported in several papers as key factors affecting cancer prognosis [43–45]. Finally, we selected 11 CRGs for analysis.

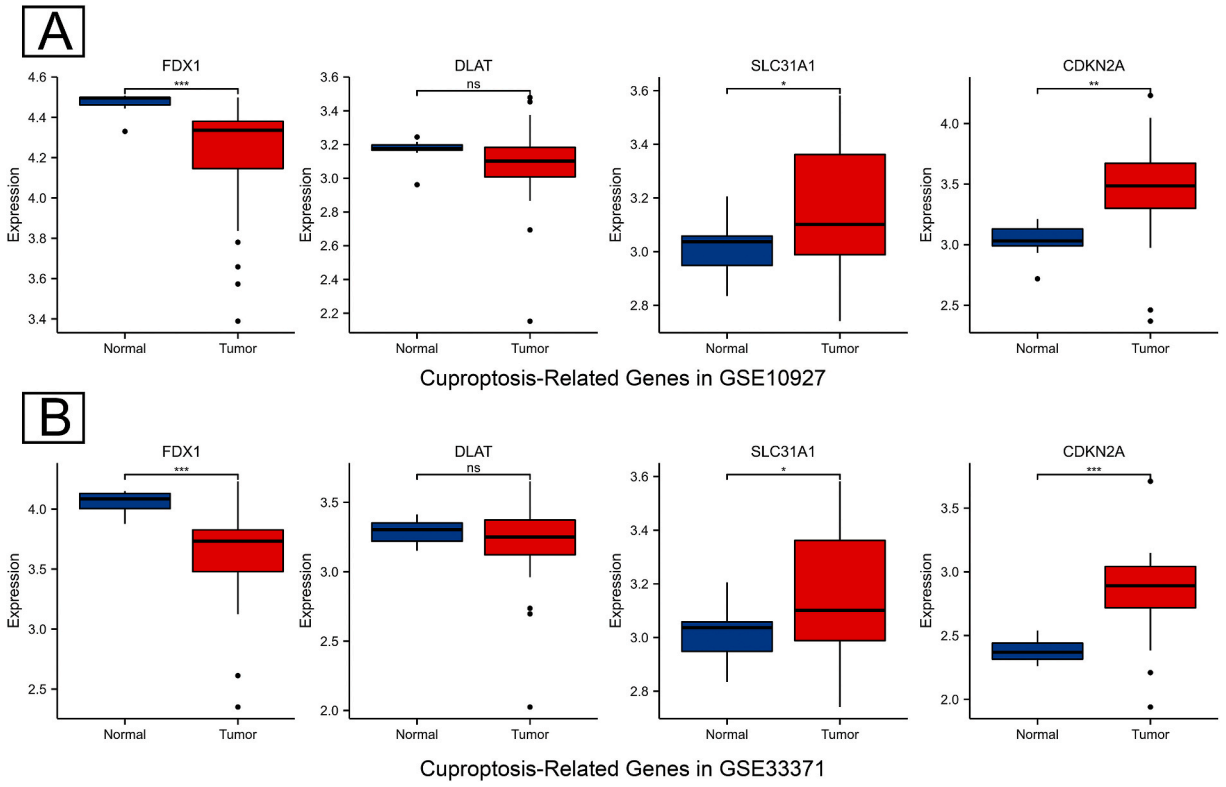

Fig. 2. Differential expression and validation of CRGs in the GEO datasets. CRG expression levels in (**A**) GSE10927 and (**B**) GSE33371. *P < 0.01, **P < 0.005, ***P < 0.001, ns: no significant differences. CRG: cuproptosis-related gene; ACC: adrenocortical carcinoma.

3.2. Differential expression and mutations of CRGs in ACC

Eleven CRGs (*FDX1*, *LIPT1*, *SLC31A1*, *MTF1*, *COX11*, *CYP2D6*, *DLAT*, *CDKN2A*, *ATP7A*,*ATP7B*, and *GCSH*) were selected for the examination of variations in gene expression between the normal and tumor tissue samples. Among these genes, only *CDKN2A* ($P < 0.001$) showed a significantly higher gene expression level in the tumor samples than in the normal tissue samples, whereas *FDX1* ($P < 0.01$), *LIPT1* ($P < 0.001$), *MTF1* ($P < 0.001$), *COX11* ($P < 0.001$), *CYP2D6* ($P < 0.001$), *ATP7B* ($P < 0.001$), and *DLAT* ($P < 0.005$) all had lower expression levels (Fig. 1A). However, the expression levels of *SLC31A1* ($P > 0.05$), *ATP7A* ($P > 0.05$), and *GCSH* ($P > 0.05$) did not differ between the two groups. Although they were shown to have a possible association with cuproptosis, we still did not include them in our follow-up analysis because they were not differentially expressed between normal adrenal tissue and ACC tissue. We computed the relevance of the different genes (Fig. 1B), of which *DLAT* and *MTF1* ($r = 0.621$, $P < 0.001$) were the most strongly correlated (Fig. 1C).

We determined the mutation rate, putative CNAs, and mRNA expression levels of the CRGs through the cBioPortal website (Fig. 1D). The significant genes with different degrees of mutation were *SLC31A1* (16 %), *ATP7A* (15 %), *CDKN2A* (12 %), and *ATP7B* (8 %). In contrast, altered mRNA expression was universal, with mRNAs highly expressed. We found that among the CNAs of the cuproptosis genes, amplifications and deep deletions were dominant in *SLC31A1* and *CDKN2A*, respectively. We found that some of the samples had missense mutations in *ATP7B*. At the same time, *CDKN2A* has specific missense and truncating mutations.

3.3. FDX1, CDKN2A, SLC31A1, and DLAT in the GEO dataset

To illustrate that the cuproptosis genes included in our model were indeed differentially expressed in separate adrenocortical

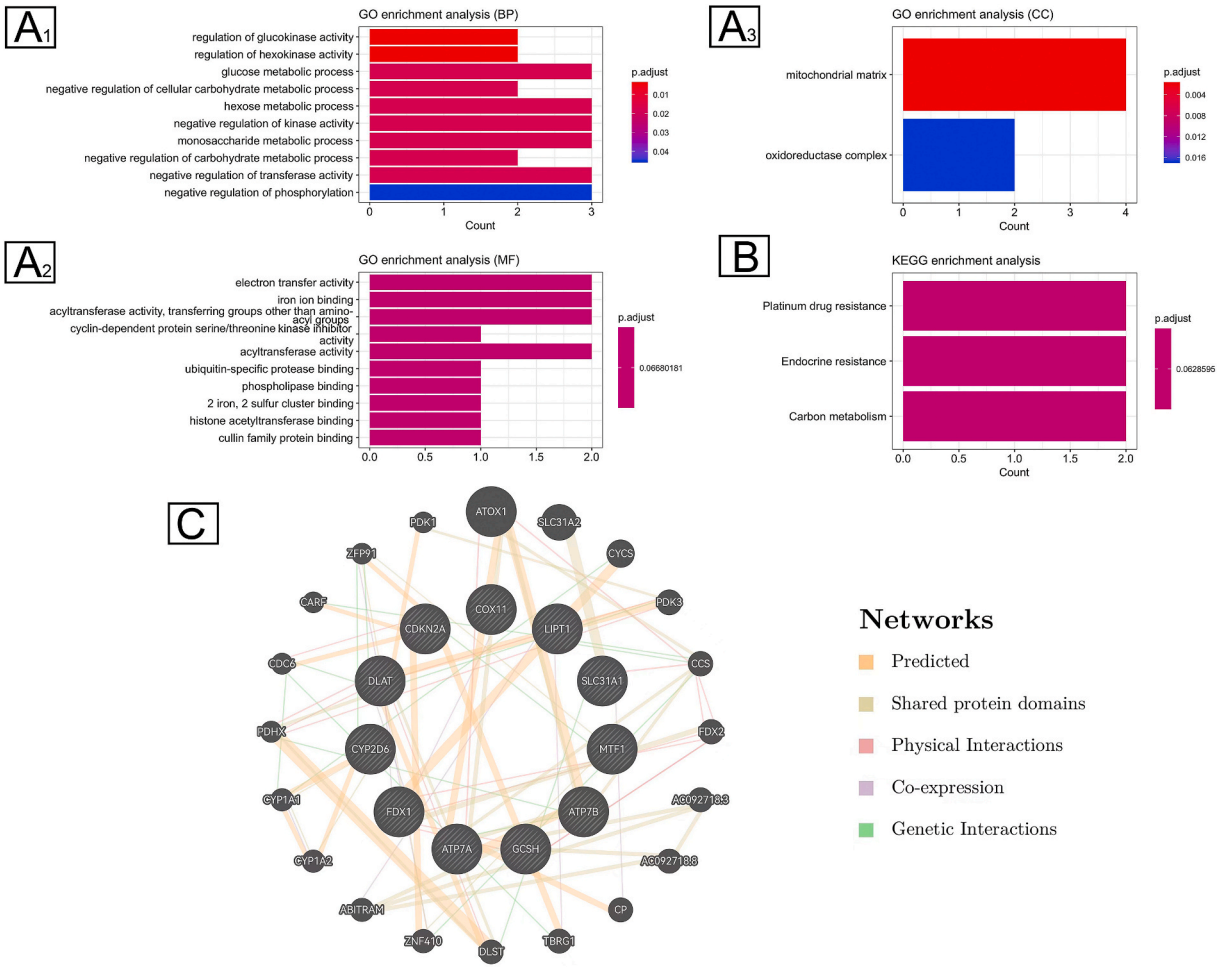

Fig. 3. Pathway enrichment and gene network analysis of the CRGs. (**A**) The enriched pathways in the Gene Ontology analysis: (**A1**) biological process (BP), (**A2**) molecular function (MF), and (**A3**) cell component (CC). (**B**) The enriched pathways in the Kyoto Encyclopedia of Genes and Genomes analysis. (**C**) CRG network analysis. FDX1, CDKN2A, DLAT, and ATP7B are the core genes. GO: Gene Ontology, KEGG: Kyoto Encyclopedia of Genes and Genomes, CRG: cuproptosis-related gene.

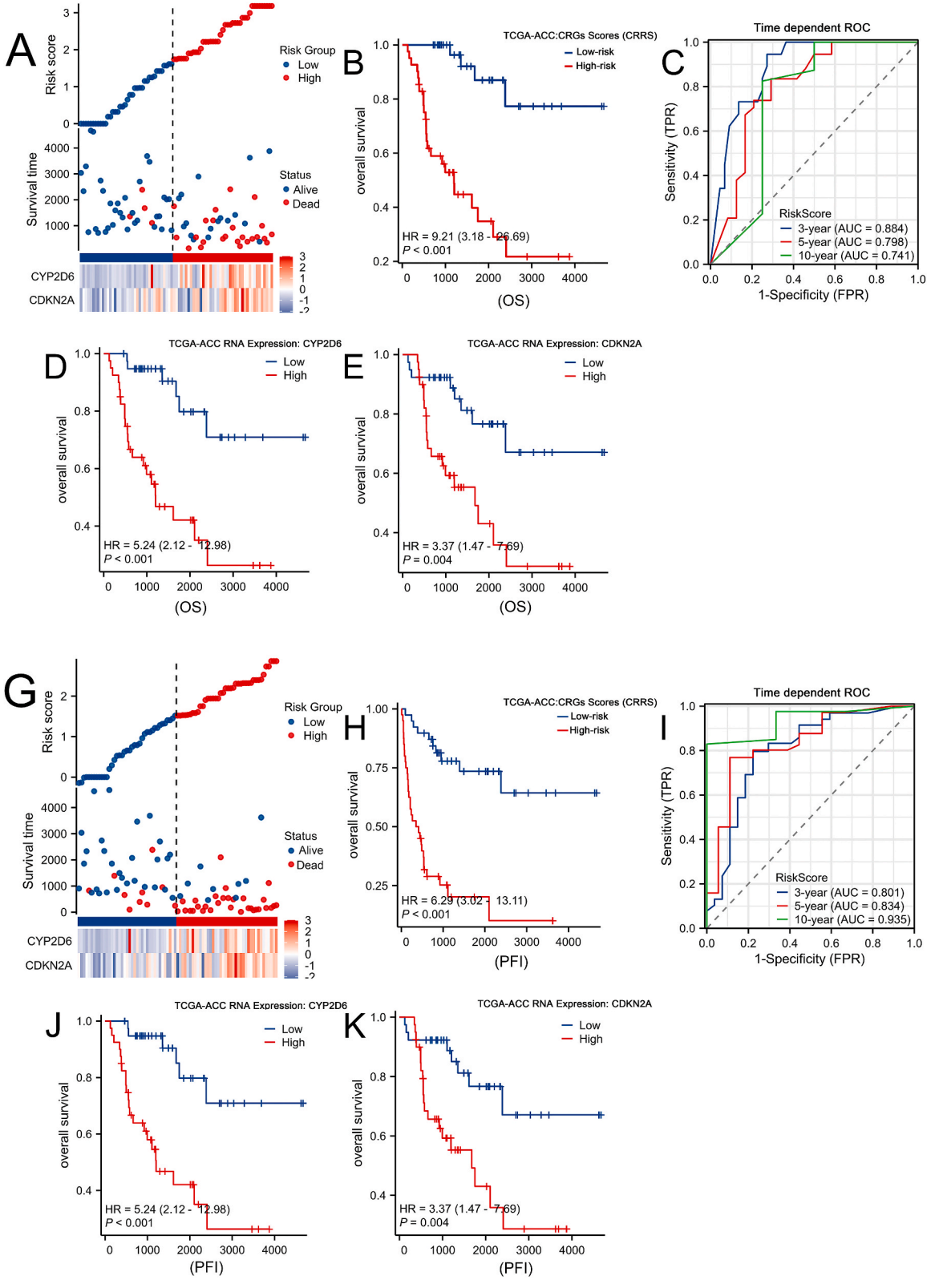

(caption on next page)

Fig. 4. Prognostic model for CRGs in ACC. OS results: (**A**) distribution diagram of the risk scores, expression levels of the CRGs, and survival statuses; (**B**) K–M plots of OS and CRRS, indicating that higher risk scores predict worse prognostic results; and (**C**) survival predictions at 3, 5, and 10 years, showing good predictive powers. The areas under the time-dependent ROC curves (AUCs) were 0.884, 0.798, and 0.741, respectively. The K–M plots for the expression levels of (**D**) CYP2D6 and (**E**) CDKN2A and OS results; (**G**) distribution diagram of risk scores, expression levels of the CRGs and survival statuses; (**H**) K–M plot of PFI and CRRS, and (**I**) survival status prediction at 3, 5, and 8 years. The AUCs were 0.801, 0.834, and 0.935, respectively. The K–M plots for the expression levels of (**J**) CYP2D6 and (**K**) CDKN2A and PFI results. OS: overall survival, PFI: progression-free interval, K–M: Kaplan–Meier, CRG: cuproptosis-related gene, ACC: adrenocortical carcinoma, ROC: receiver-operating characteristic.

cancer samples, we included two datasets (GSE10927 [Fig. 2A], GSE33371 [Fig. 2B]) from the GEO database for analysis. A total of 10 human normal adrenal cortex tissue samples and 33 human ACC samples were registered in the GSE10927 database. The GSE33371 database contained another 10 normal and 33 tumor tissue samples. In the two GEO datasets, we observed differential expression of *FDX1* ($P < 0.001$), *SLC31A1* ($P < 0.05$), and *CDKN2A* ($P < 0.001$), whereas the difference in *DLAT* expression was not significant. These results were generally consistent with the expression differences in the TCGA-ACC database. We selected the genes described in the following sections as sources for analysis, revealing their different biological roles.

3.4. Pathway enrichment and gene network analysis of CRGs

Using the GO database, we identified the target genes that were mainly associated with the cell component (CC), molecular function (MF), and biological process (BP) levels. The organic processes related to the CRGs in the GO analysis were the generation of precursor metabolites and energy; regulation of macrophage apoptotic process; acetyl-CoA biosynthetic process from pyruvate; and mitochondrial matrix (Fig. 3 A1-A3). Moreover, the CRGs correlated with endocrine resistance and platinum drug resistance in the KEGG analysis (Fig. 3B). In the protein–protein interaction (PPI) analysis [46], we found that the core genes were *FDX1*, *CDKN2A*,

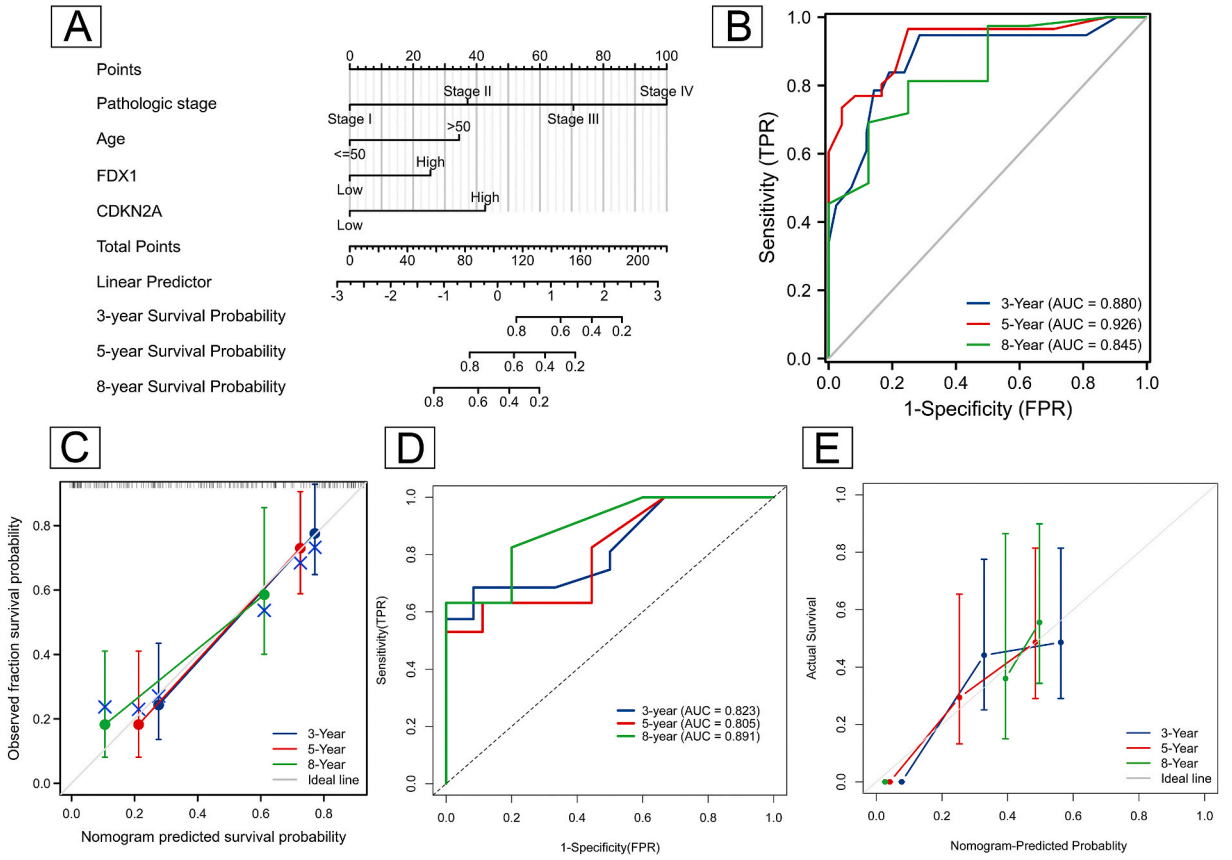

Fig. 5. Development of the nomogram model and independent cohort validation. The nomogram model predicts the 3-, 5-, and 8-year OS (**A**), including the differential expression levels of FDX1 and CDKN2A, pathological stage, and age of onset. The time-dependent ROC curves (**B**) for OS and calibration curves (**C**) show that our model has superior prognosis predictive results in patients with ACC. In the independent cohorts GSE33371 and GSE10927, the time-dependent ROC curves (**D**) and calibration curves (**E**) demonstrated the reliable generalization of our constructed prognostic nomogram. OS: overall survival, ACC: adrenocortical carcinoma, AUC: area under the time-dependent ROC curve, TPR: true positive rate, FPR: false positive rate.

DLAT, and *ATP7B* (Fig. 3C).

3.5. Establishment of a prognostic model involving CRGs for ACC

We constructed a model to further explore the link between CRG expression and prognosis and to predict the 3-, 5-, and 10-year prognosis of patients with ACC. In the univariate Cox regression analysis of OS, we found that the CRGs *FDX1* (HR = 2.307; 95 % CI: 1.041–5.113; P = 0.033), *CDKN2A* (HR = 4.155; 95 % CI: 1.758–9.842; P < 0.001), *LIPT1* (HR = 3.032; 95 % CI: 1.332–6.903; P = 0.008), *CYP2D6* (HR = 5.241; 95 % CI: 2.116–12.980; P < 0.001) and *DLAT* (HR = 2.172 95 % CI: 1.000–4.716; P = 0.050) were significantly correlated (Table S1). In contrast, only *ATP7B* (HR = 1.590 95 % CI: 0.853–2.962; P = 0.144) was not associated with PFI in the univariate Cox regression analysis (Table S2). In the multivariate analysis of OS, we identified *CDKN2A* (HR = 2.620; 95 % CI: 1.017–6.750; P = 0.046) and *CYP2D6* (HR = 3.489; 95 % CI: 1.349–9.021; P = 0.010). In the PFI analysis, *CDKN2A* (HR = 2.204; 95 % CI: 1.071–4.532; P = 0.032) and *CYP2D6* (HR = 2.208; 95 % CI: 1.006–4.843; P = 0.048) remained statistically significant. In comparison, *CDKN2A* and *CYP2D6* were related to worse prognosis. However, a large amount of research data is needed to support these findings.

In our prognostic model, we used the R package "survival" to construct the relevant prognostic profiles of patients with ACC. We selected two representative genes (*CDKN2A* and *CYP2D6*) for OS (Fig. 4A) and PFI (Fig. 4G) to establish a CRRS map. In our study, higher risk scores were significantly associated with poor OS (HR = 9.21; 95 % CI: 3.18–26.69; P < 0.001) (Fig. 4B) and PFI (HR = 6.29; 95 % CI: 3.02–13.11; P < 0.001) (Fig. 4H). Moreover, in the OS and PFI models for patients with ACC, the AUC at 3, 5, and 10 years was used to assess the predictive power for survival outcomes. The AUCs were 0.869, 0.818, and 0.848 for the OS outcomes of patients with ACC (Figs. 4C), 0.801 and 0.834, and 0.935 for PFI outcomes (Fig. 4I), both of which showed good results. The K–M plots for the expression levels of *CYP2D6* and *CDKN2A* and OS(Fig. 4**D-E**), PFI (Fig. 4**J-K**) results.In summary, the model we used had accurate predictive strength and was considerably associated with the survival time of patients with ACC.

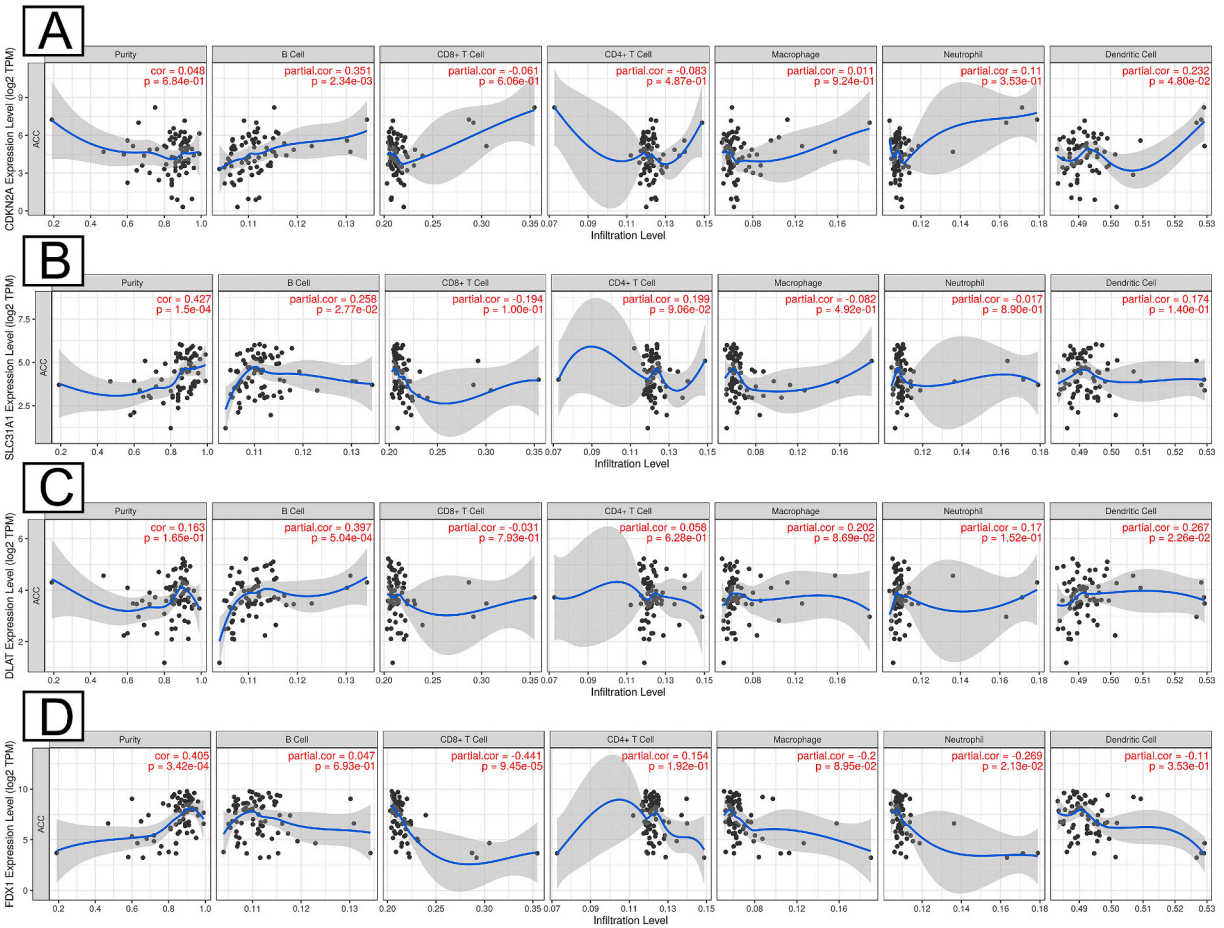

Fig. 6. Correlation between the expression of CDKN2A (**A**), SLC31A1 (**B**), DLAT (**C**), and FDX1 (**D**) and immune infiltration levels. Cor: correlation.

3.6. Development and external Verification of the predictive nomogram model

Considering the clinical stage of patients with ACC, the differences in age of onset, sex, and the clinical application of the model, we developed a nomogram model to assist clinicians in providing a better assessment of the survival of patients with ACC (Fig. 5A). We used univariate and multivariate Cox regressions to analyze clinical data from TCGA (Table S3) and performed an internal validation of this model. The results showed that clinical stage and *FDX1* and *CDKN2A* expression levels were independent prognostic factors for OS. The calculated C-index was 0.806, indicating the superb predictive performance of our model. Simultaneously, we assessed the specificity and sensitivity of the OS results by using time-dependent ROC and calibration curves (Fig. 5B and C), and the plots showed good results. On the basis of the data generated, the area under the ROC curve (AUROC) for OS was 0.880, 0.926, and 0.845 at 3, 5, and 8 years, respectively. We also applied independent cohorts (GSE33371 and GSE10927) for external validation. Similarly, in the validation cohort from the GEO database (Fig. 5D-E), the AUCs for 3-, 5-, and 8-year OS were 0.823, 0.805, and 0.891, respectively, demonstrating good generalization of our nomogram model.

3.7. Association between CRGs and immune infiltration in Organisms

We analyzed the gene expression data from the TCGA database to infer the abundances of tumor-infiltrating immune cells. B cells, $CD8^+$ T cells, $CD4^+$ T cells, macrophages, dendritic cells, and neutrophils were analyzed to establish the relationship between tumor-associated immunity and the expression of CRGs (*CDKN2A*, *SLC31A1*, *DLAT*, and *FDX1*) (Fig. 6A–D). We found that *CDKN2A* expression positively correlated with B-cell ($P = 2.43 \times 10^{-3}$) and dendritic cell ($P = 4.80 \times 10^{-2}$) immune infiltration levels. A negative correlation was found between *FDX1* expression and the immune infiltration levels of $CD8^+$ T cells ($P = 9.45 \times 10^{-5}$) and

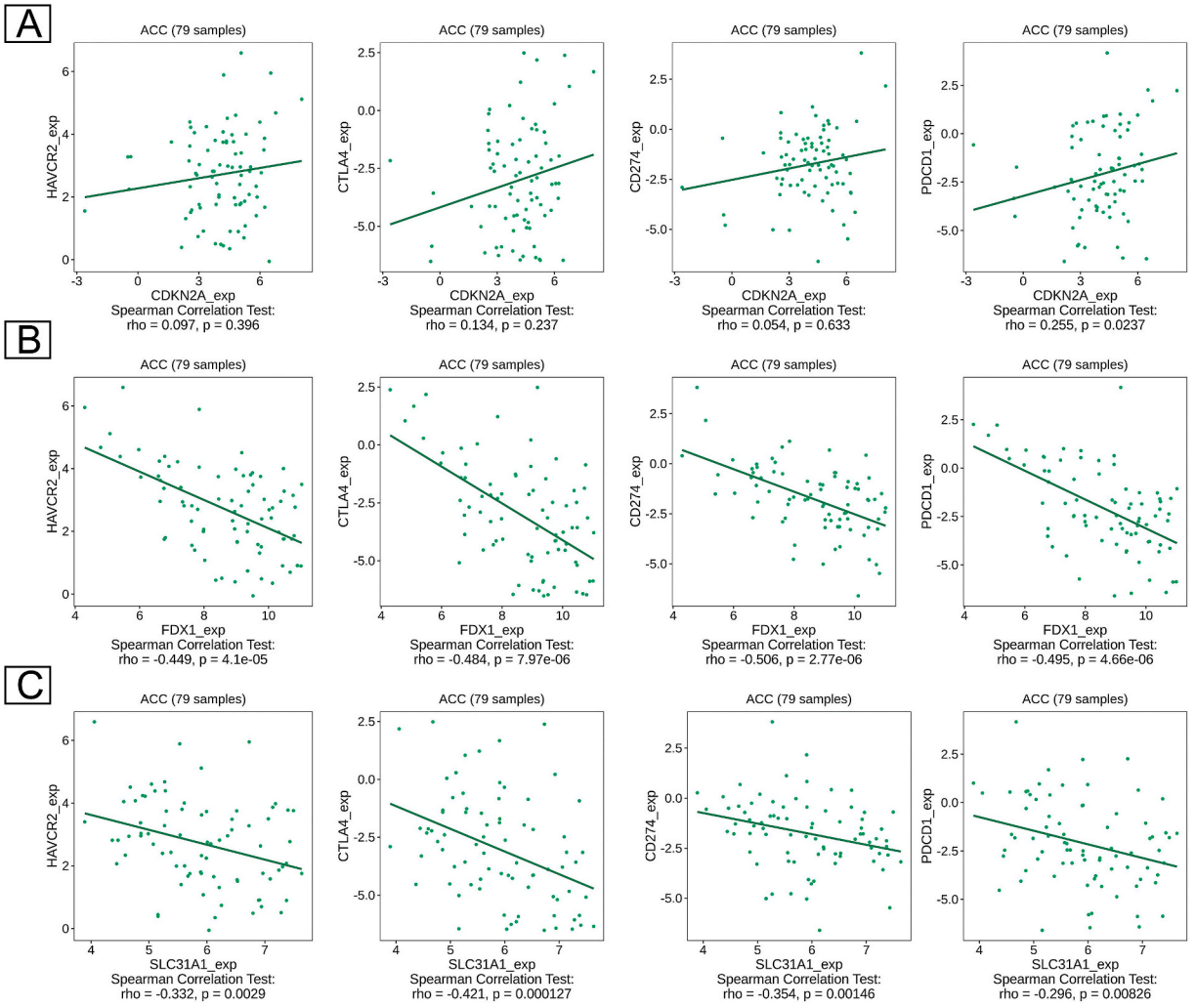

Fig. 7. Correlation between the expression of (**A**) CDKN2A, (**B**) FDX1, and (**C**) SLC31A1 and the immune checkpoints HAVCR2, CTLA-4, CD274, and PDCD1 in patients with ACC. ACC: adrenocortical carcinoma, Exp: expression.

neutrophils ($P = 2.13 \times 10^{-2}$). A positive correlation was found between *SLC31A1* and B-cell immune infiltration levels ($P = 2.77 \times 10^{-2}$) and between *DLAT* expression and B-cell ($P = 5.04 \times 10^{-4}$) and dendritic cell immune infiltration levels ($P = 2.26 \times 10^{-2}$).

Immune checkpoints are a normal part of the body's immune system, preventing the body from developing an overly strong immune response to its tissues. Through this mechanism, cancer cells inhibit immune cell function and thus evade clearance by the autoimmune system, which can be undone by ICIs. We investigated the connection between the expression of the CRGs and immune checkpoints. Our study showed a significant positive correlation between *CDKN2A* and *PD-1* expression levels ($r = 0.255$, $P = 0.0237$) (Fig. 7A). *FDX1* expression was negatively correlated with the expression levels of *PD-L1* ($r = -0.506$, $P = 2.77 \times 10^{-6}$), *PD-1* ($r = -0.495$, $P = 4.66 \times 10^{-6}$), *CTLA-4* ($r = -0.484$, $P = 7.97 \times 10^{-6}$), and *TIM-3* ($r = -0.449$, $P = 4.10 \times 10^{-5}$) (Fig. 7B). *SLC31A1* was also negatively correlated with the expression levels of *PD-L1* ($r = -0.354$, $P = 1.46 \times 10^{-3}$), *PD-1* ($r = -0.296$, $P = 8.26 \times 10^{-3}$), *CTLA-4* ($r = -0.421$, $P = 1.27 \times 10^{-4}$), and *TIM-3* ($r = -0.332$, $P = 0.29 \times 10^{-3}$) (Fig. 7C).

4. Discussion

The mechanism of cuproptosis depends on the accumulation of copper ions. Cuproptosis is associated with disease onset and progression, indicating that it is a potential cancer prevention and treatment pathway [47]. Copper ions act directly on the TCA cycle and ultimately induce cell death. Our study detailed the association of three key CRGs (*FDX1*, *CDKN2A*, and *CYP2D6*) with prognosis in patients with ACC and demonstrated that these three genes are risk variations for ACC, with higher risk scores linked to a poorer prognosis.

In this study, we used the TCGA-ACC database to investigate the expression variations and mutational characteristics of CRGs. Most differences in the CRGs were comparable with those reported in previous research studies, in contrast to other cancer types [45,48,49]. We also performed prognostic analyses (OS, PFI), nomogram evaluation, immune infiltration, and other analyses. All findings were equally significant. As described earlier, the CRRS and nomogram models were significantly associated with the clinicopathological characteristics of ACC. The data suggest that the models represent independent factors in the survival outcome of patients with ACC. Likewise, the ROC curve values and validation analyses showed that the models have good predictive powers. For this reason, we believe that our models have predictive value in clinical care for evaluating patients with ACC and determining their survival expectations.

Copy number variants (CNVs) play an important role in cancer development and progression due to rearrangements (e.g., chromosomal deletions, duplications, insertions, and translocations) in the cancer genome that result in the amplification or deletion of chromosomal segments. Correspondingly, deletions and amplifications at the DNA level are reflected at the RNA level by differences in RNA expression. According to information from the TCGA database and the cBioPortal website, most patients had high expression of CRGs at the mRNA level. In *CDKN2A*, the main mutation type of the gene was a deep deletion, which was different from the other genes.

Next, we used CRGs to study the correlation with cuproptosis using the ACC as the subject. Three CRGs, namely, *FDX1*, *CYP2D6*, and *CDKN2A*, have different biochemical effects. *FDX1* is highly correlated with the expression levels of lipoylated proteins [18], which encode an iron-sulfur protein and convert Cu^{2+} to Cu^{1+} [49]. It is also an upstream regulator of the TCA cycle, and inhibiting its expression contributes to cellular freedom from copper toxicity [49,50]. *CYP2D6*, an isoenzyme of cytochrome P450, is the key enzyme in the metabolism of N-methyltamoxifen to endoxifen. Scientific studies have shown that *CYP2D6* is polymorphic and that different genotypes of *CYP2D6* metabolize tamoxifen at different levels and produce different concentrations of the active metabolite endoxifen [51]. Patients with low endoxifen concentrations (<14 nM) had a higher risk of distant recurrence or death than patients with high concentrations (>35 nM) [51]. Moreover, the function of *CDKN2A* is connected with cell cycle regulation and has been linked to the improvement of the outcomes of several tumors [52–54]. *CDKN2A* encodes a protein that binds to cyclin-dependent kinases 4 and 6 (*CDK4/6*) to stop the cell cycle in the gap phase and regulate the cell cycle. In a previous study, a patient presented with mutations in *CDKN2A* and *CDKN2B* [52], which allowed cells to proliferate indefinitely, leading to disease development [52,53]. This suggests that treatment targeting the cell cycle pathway may benefit some patients. In recent years, related studies have found that ICIs are effective in many tumors, including lung cancer and melanoma [55]. As we described and as Shi et al. [55] revealed, practical markers for distinguishing ACC patients with potential sensitivity to immunotherapy are still lacking.

Further studies have shown that programmed cell death-1 (*PD-1*) is an immune checkpoint receptor expressed by T cells [56], while programmed cell death ligands-1 and 2 (*PD-L1* and *PD-L2)* are expressed in the microenvironment of some cancers. A systematic study estimated that 11 % of ACC patients showed *PD-L1* expression on tumor cell membranes [57], while 70 % of tumor-infiltrating monocytes were *PD-L1*-positive. We also know that *PD-1* is a key factor in tumor development. Higher expression of *PD-1* was found to be associated with worse prognosis. Our study validates the relationship between CRGs and four immune checkpoints (*PD-1*, *PD-L1*, *CTLA-4*, and *TIM-4*). We found that *CDKN2A* expression positively correlated with the *PD-1* expression level. A general study found that overexpression of immune checkpoints, especially *PD-1/L1* and *CTLA4*, produces signals that inhibit T-cell function and thus suppress the antitumor immune process [7]. This may indicate the relevance of *CDKN2A* expression to the immune escape mechanism of tumors. However, there is a contradiction in the efficacy of the effect of *CDKN2A/2B* deletion on *PD-1/PD-L1*, as one recent study suggests that deletion of this gene can lead to rapid tumor progression when *PD-1/PD-L1*-based therapy is administered {Chen, 2022 #64}, while another opposing view suggests that *CDKN2A/2B* not only does not lead to progression but also promotes the efficacy of immunotherapy. In our study, we found that *CDKN2A* expression was higher in tumor tissues than in normal adrenal tissues, and similarly, higher *CDKN2A* expression was associated with worse scores and prognosis, leading us to speculate that the application of PD-1/PD-L1 treatment may have good efficacy in patients with ACC. Our conclusions are supported by several relevant studies that found that the PD-1 inhibitor pembrolizumab provided clinically significant and durable antitumor activity with a manageable safety

profile in patients with advanced ACC [58]{Raj, 2020 #69}. In a retrospective study, a 50 % disease control rate was achieved in patients who received cabozantinib (a multikinase inhibitor), showing relatively good efficacy [59]. These findings suggest that ACC has some sensitivity to ICIs [54], and some case reports have indicaated the therapeutic advantage of administering ICIs to patients with ACC [60].

The immune response performs a dominant function in tumorigenesis and is regularly used as a target for tumor therapy [43]. Our study found that *CDKN2A* expression positively correlated with the immune infiltration levels of B cells and dendritic cells. In contrast, *FDX1* expression was negatively correlated with the levels of infiltrating $CD8^+$ T cells and neutrophils. We found that immune infiltration was associated with ACC patient survival [61]. This conclusion was correlated with our findings in B cells only. This also provides a potential target for future clinical drug development [62]. Therapeutic research in ACC has identified various emerging treatment approaches [54], but no targeted agents have been approved for the treatment of ACC.

In a study investigating the way in which immune cell infiltration in the tumor microenvironment changes with tumor progression, Sierra et al. found that the increase in the levels of NK cells inhibited the proliferation of CD8 T cells in an in vitro experiment with a multicellular line, and the experiment demonstrated that cell infiltration may impair the body's immune regulatory function. The various factors these cells produce play a central role in the tumor microenvironment, driving immune-mediated tumor activity in the tumor microenvironment. T cells are important effectors of the body's immune system in the fight against cancer and are divided into $CD8^+$ T cells and $CD4^+$ T cells. Usually, only $CD8^+$ T cells are considered to have tumor-eliminating effects, but clinical studies have found that $CD4^+$ T cells in tumors are also cytotoxic [62]. $CD8^+$ T cells normally kill infected or mutation-producing tumor cells by secreting a considerable amount of IFN-γ and the protease granzyme B. In contrast, $CD4^+$ T cells activate $CD8^+$ T cells after the initiation of cellular immunity through several mechanisms to differentiate them into cytotoxic T lymphocytes (CTLs), and they have also been found to have a role in maintaining and enhancing the antitumor response of CTLs. However, even in the absence of $CD8^+$ T cells, $CD4^+$ T cells can also kill tumor cells directly by an IFN-γ-related mechanism. This illustrates the critical role of $CD4^+$ T cells in tumor immunity. However, we found that the relationship between tumor tissues with high *CDKN2A* gene expression and low *FDX1* gene expression and the number of $CD4^+$ T cells was not statistically significant. In addition, the number of $CD8^+$ T cells in the tumor microenvironment was inversely correlated with FDX1 expression in our analysis of the samples, and the gene expression of FDX1 was significantly lower in tumor tissues than in normal tissues, suggesting that more $CD8^+$ T cells may be produced in tumor tissues. We speculate that FDX1 suppresses $CD8^+$ T-cell expression, which reduces immune cell infiltration of cancerous tissues in patients with ACC, leading to a worse prognosis. Similar to the abovementioned related study, $CD8^+$ T cells have a tumor-killing effect, and patients with tumors with a better prognosis have more immune cell infiltration of the tumor microenvironment; as a result, patients may respond better to cancer immunotherapy. Our finding that low expression of FDX1 correlates with better prognosis is consistent with this study. In a follow-up study, we aim to further elucidate this mechanism. By studying cytotoxic $CD4^+$ and $CD8^+$ T cells, more innovative and effective immunotherapies may be developed.

However, there are some shortcomings in our study. First, we extracted secondary data from the TCGA database, which might have potential selection bias. A large amount of data is needed to validate our model and make better predictions. Second, although the CRRS model we constructed had considerable predictive power, we only partially considered factors associated with ACC prognosis. In the future, we should design more targeted prospective studies to make our model more convincing. However, we are limited by time and venue conditions. We did not choose to perform wet lab validation experiments with ACC cell lines, which is a limitation. In future investigations, we aim to conduct further studies on ACC, and cellular assays and clinical studies are the next step in our research.

5. Conclusions

In conclusion, our models systematically analyzed the relationship between CRGs and ACC and clarified that cuproptosis plays an essential role in ACC outcomes. The CRRS and nomogram models we developed were confirmed to have excellent prognostic predictive abilities in patients with ACC. Therefore, an in-depth evaluation of patients with CRRS rankings is clinically essential and can assist in further therapy in the future.

Data availability statement

The data relevant to our study were obtained from publicly available repositories. We declare that these data are available in public repositories.

Our data were obtained from the TCGA-ACC and GTEx-ACC datasets and the GEO database GSE10927 and GSE33371 datasets.

CRediT authorship contribution statement

Zhiyuan You: Writing - review & editing, Writing - original draft, Visualization, Validation, Methodology, Investigation, Funding acquisition, Formal analysis, Data curation, Conceptualization. **Jiqing He:** Writing - review & editing, Project administration. **Zhongming Gao:** Writing - review & editing, Supervision, Formal analysis.

Declaration of competing interest

The authors declare that they have no known competing financial interests or personal relationships that could have appeared to influence the work reported in this paper.

Appendix A. Supplementary data

Supplementary data to this article can be found online at https://doi.org/10.1016/j.heliyon.2023.e23661.

References

[1] J.F.H. Pittaway, L. Guasti, Pathobiology and genetics of adrenocortical carcinoma, J. Mol. Endocrinol. (2) (2019) 62. R105–R119.
[2] M. Fassnacht, et al., *Adrenocortical carcinoma: a clinician's update.* Nat. Rev, Endocrinol. 7 (6) (2011) 323–335.
[3] J.H. Heaton, et al., Progression to adrenocortical tumorigenesis in mice and humans through insulin-like growth factor 2 and β-catenin, Am. J. Pathol. 181 (3) (2012) 1017–1033.
[4] Y. Cheng, et al., Future directions in diagnosis, prognosis and disease monitoring of adrenocortical carcinoma: novel non-invasive biomarkers, Front. Endocrinol. 12 (2021) 811293.
[5] M.L. Kendrick, et al., Aldosterone-secreting adrenocortical carcinomas are associated with unique operative risks and outcomes, Surgery 132 (6) (2002) 1008–1011, discussion 1012.
[6] C. Scollo, et al., Prognostic factors for adrenocortical carcinoma outcomes, Front. Endocrinol. 7 (2016) 99.
[7] C. Jimenez, et al., Endocrine and neuroendocrine tumors special issue-checkpoint inhibitors for adrenocortical carcinoma and metastatic pheochromocytoma and paraganglioma: do they work? Cancers 14 (3) (2022) 467.
[8] F. Focarelli, A. Giachino, K.J. Waldron, Copper microenvironments in the human body define patterns of copper adaptation in pathogenic bacteria, PLoS Pathog. 18 (7) (2022), e1010617.
[9] X. Ding, et al., Analysis of serum levels of 15 trace elements in breast cancer patients in Shandong, China, Environ. Sci. Pollut. Res. Int. 22 (10) (2015) 7930–7935.
[10] V. Pavithra, et al., Serum levels of metal ions in female patients with breast cancer, J. Clin. Diagn. Res. (1) (2015) 9. BC25–BC27.
[11] X. Zhang, Q. Yang, Association between serum copper levels and lung cancer risk: a meta-analysis, J. Int. Med. Res. 46 (12) (2018) 4863–4873.
[12] F. Michniewicz, et al., *Copper: an intracellular achilles' heel allowing the targeting of epigenetics, kinase pathways, and cell metabolism in cancer therapeutics.* ChemMedChem 16 (15) (2021) 2315–2329.
[13] V. Oliveri, Selective targeting of cancer cells by copper ionophores: an overview, Front. Mol. Biosci. 9 (2022) 841814.
[14] M.V. Babak, D. Ahn, Modulation of intracellular copper levels as the mechanism of action of anticancer copper complexes: clinical relevance, Biomedicines 9 (8) (2021) 852.
[15] T. Vanden Berghe, et al., *Regulated necrosis: the expanding network of non-apoptotic cell death pathways.* Nat. Rev. Mol, Cell Biol. 15 (2) (2014) 135–147.
[16] W. Wang, et al., The cuproptosis-related signature associated with the tumor environment and prognosis of patients with glioma, Front. Immunol. 13 (2022) 998236.
[17] M. Xie, et al., Cuproptosis-related MiR-21-5p/FDX1 axis in clear cell renal cell carcinoma and its potential impact on tumor microenvironment, Cells 12 (1) (2022) 173.
[18] P. Tsvetkov, et al., Copper induces cell death by targeting lipoylated TCA cycle proteins, Science 375 (6586) (2022) 1254–1261.
[19] D. Denoyer, et al., Targeting copper in cancer therapy: 'copper that cancer', Metallomics 7 (11) (2015) 1459–1476.
[20] J.L. Allensworth, et al., *Disulfiram (DSF) acts as a copper ionophore to induce copper-dependent oxidative stress and mediate anti-tumor efficacy in inflammatory breast cancer.* Mol. Oncol 9 (6) (2015) 1155–1168.
[21] T. Wang, et al., *Cuproptosis-related gene FDX1 expression correlates with the prognosis and tumor immune microenvironment in clear cell renal cell carcinoma.* Front, Immunol. 13 (2022) 999823.
[22] Z. Cai, et al., Cuproptosis-related modification patterns depict the tumor microenvironment, precision immunotherapy, and prognosis of kidney renal clear cell carcinoma, Front. Immunol. 13 (2022) 933241.
[23] H. Yuan, et al., *The cuproptosis-associated 13 gene signature as a robust predictor for outcome and response to immune- and targeted-therapies in clear cell renal cell carcinoma.* Front, Immunol. 13 (2022) 971142.
[24] S. Xin, et al., *A cuproptosis-related lncRNA signature identified prognosis and tumour immune microenvironment in kidney renal clear cell carcinoma.* Front. Mol, Biosci. 9 (2022) 974722.
[25] K. Li, et al., Cuproptosis identifies respiratory subtype of renal cancer that confers favorable prognosis, Apoptosis 27 (11–12) (2022) 1004–1014.
[26] G. Zhang, et al., Cuproptosis status affects treatment options about immunotherapy and targeted therapy for patients with kidney renal clear cell carcinoma, Front. Immunol. 13 (2022) 954440.
[27] Y. Cai, et al., Comprehensive analysis of the potential cuproptosis-related biomarker LIAS that regulates prognosis and immunotherapy of pan-cancers, Front. Oncol. 12 (2022) 952129.
[28] H.J. Yuan, Y.T. Xue, Y. Liu, *Cuproptosis, the novel therapeutic mechanism for heart failure: a narrative review.* Cardiovasc, Diagn. Ther. 12 (5) (2022) 681–692.
[29] L. Chen, J. Min, F. Wang, Copper homeostasis and cuproptosis in health and disease, Signal Transduct. Target. Ther. 7 (1) (2022) 378.
[30] C. Xiong, et al., Cuproptosis: p53-regulated metabolic cell death? Cell Death Differ. 30 (4) (2023) 876–884.
[31] J. Xie, et al., *Cuproptosis: mechanisms and links with cancers.* Mol, Cancer 22 (1) (2023) 46.
[32] T.J. Giordano, et al., Molecular classification and prognostication of adrenocortical tumors by transcriptome profiling, Clin. Cancer Res. 15 (2) (2009) 668–676.
[33] J. Vivian, et al., *Toil enables reproducible, open source, big biomedical data analyses.* Nat, Biotechnol. 35 (4) (2017) 314–316.
[34] F. Wang, et al., *Cuproptosis-related lncRNA predict prognosis and immune response of lung adenocarcinoma.* World J, Surg. Oncol. 20 (1) (2022) 275.
[35] S. Zhang, et al., *A cuproptosis and copper metabolism-related gene prognostic index for head and neck squamous cell carcinoma.* Front, Oncol. 12 (2022) 955336.
[36] M. Franz, et al., GeneMANIA update 2018, Nucleic Acids Res. (W1) (2018) 46. W60–W64.
[37] G. Yu, et al., *clusterProfiler: an R package for comparing biological themes among gene clusters.* Omics 16 (5) (2012) 284–287.
[38] Gene Ontology Consortium, Gene ontology consortium: going forward, Nucleic Acids Res. (Database issue) (2015) 43. D1049–D56.
[39] M. Kanehisa, S. Goto, KEGG: kyoto encyclopedia of genes and genomes, Nucleic Acids Res. 28 (1) (2000) 27–30.
[40] T. Li, et al., TIMER: a web server for comprehensive analysis of tumor-infiltrating immune cells, Cancer Res. (21) (2017) 77, e108–e110.
[41] Y. Fan, et al., Hepcidin upregulation in lung cancer: a potential therapeutic target associated with immune infiltration, Front. Immunol. 12 (2021) 612144.
[42] B. Ru, et al., *TISIDB: an integrated repository portal for tumor-immune system interactions.* Bioinformatics 35 (20) (2019) 4200–4202.
[43] Q. Song, et al., Cuproptosis scoring system to predict the clinical outcome and immune response in bladder cancer, Front. Immunol. 13 (2022) 958368.
[44] Y. Huang, D. Yin, L. Wu, Identification of cuproptosis-related subtypes and development of a prognostic signature in colorectal cancer, Sci. Rep. 12 (1) (2022) 17348.
[45] Q. Hu, et al., Cuproptosis predicts the risk and clinical outcomes of lung adenocarcinoma, Front. Oncol. 12 (2022) 922332.
[46] Y. Wang, et al., The hippo pathway effector transcriptional co-activator with PDZ-binding motif correlates with clinical prognosis and immune infiltration in colorectal cancer, Front. Med. 9 (2022) 888093.
[47] V.C. Shanbhag, et al., Copper metabolism as a unique vulnerability in cancer, Biochim. Biophys. Acta Mol. Cell Res. 1868 (2) (2021) 118893.
[48] Y. Yun, et al., Cuproptosis-related gene - SLC31A1, FDX1 and ATP7B - polymorphisms are associated with risk of lung cancer, Pharmgenomics Pers. Med. 15 (2022) 733–742.

[49] Z. Bian, R. Fan, L. Xie, *A novel cuproptosis-related prognostic gene signature and validation of differential expression in clear cell renal cell carcinoma.* Genes (Basel) 13 (5) (2022) 851.
[50] B. Dörsam, J. Fahrer, The disulfide compound α-lipoic acid and its derivatives: a novel class of anticancer agents targeting mitochondria, Cancer Lett. 371 (1) (2016) 12–19.
[51] M.P. Goetz, et al., Clinical pharmacogenetics implementation consortium (CPIC) guideline for CYP2D6 and tamoxifen therapy, Clin. Pharmacol. Ther. 103 (5) (2018) 770–777.
[52] H. Kimura, et al., The role of inherited pathogenic CDKN2A variants in susceptibility to pancreatic cancer, Pancreas 50 (8) (2021) 1123–1130.
[53] J.M. Lavoie, et al., Whole-genome and transcriptome analysis of advanced adrenocortical cancer highlights multiple alterations affecting epigenome and DNA repair pathways. Cold Spring Harb, Mol. Case Stud (3) (2022) 8, a006148.
[54] B. Nazha, et al., Blood-based next-generation sequencing in adrenocortical carcinoma, Oncol. 27 (6) (2022) 462–468.
[55] X. Shi, et al., Cancer stemness associated with prognosis and the efficacy of immunotherapy in adrenocortical carcinoma, Front. Oncol. 11 (2021) 651622.
[56] A.N. Araújo, M.J. Bugalho, *Advanced adrenocortical carcinoma: current perspectives on medical treatment.* Horm, Metab. Res. 53 (5) (2021) 285–292.
[57] L. Khoja, et al., *Pembrolizumab.* J. ImmunoTher, Cancer 3 (1) (2015) 36.
[58] N. Raj, et al., *PD-1 blockade in advanced adrenocortical carcinoma.* J, Clin. Oncol. 38 (1) (2020) 71–80.
[59] M. Kroiss, et al., Objective response and prolonged disease control of advanced adrenocortical carcinoma with cabozantinib, J. Clin. Endocrinol. Metab. 105 (5) (2020) 1461–1468.
[60] J. Lang, et al., Development of an adrenocortical cancer humanized mouse model to characterize anti-PD1 effects on tumor microenvironment, J. Clin. Endocrinol. Metab. 105 (1) (2020) 26–42.
[61] K. Yuan, et al., Identification and verification of immune-related genes prognostic signature based on ssGSEA for adrenocortical carcinoma (ACC), Int. J. Gen. Med. 15 (2022) 1471–1483.
[62] D.Y. Oh, L. Fong, Cytotoxic $CD4^+$ T cells in cancer: expanding the immune effector toolbox, Immunity 54 (12) (2021) 2701–2711.